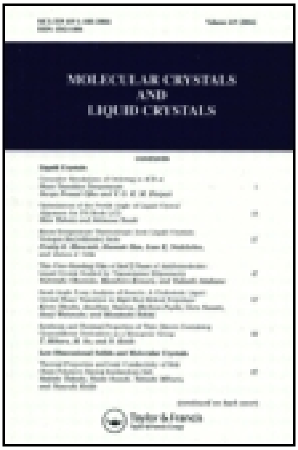

Molecular Crystals and Liquid Crystals
Publication details, including instructions for authors and subscription information:
http://www.tandfonline.com/loi/gmcl20

Measurement of Flexoelectric Coefficients in Nematic Liquid Crystals Using Shallow Grating Devices

Hanna M. Sykulska [a], Lesley A. Parry-Jones [a] & Steve J. Elston [a]

[a] Department of Engineering Science, Oxford University, Parks Road, Oxford, United Kingdom

Version of record first published: 31 Aug 2006

Mol. Cryst. Liq. Cryst., Vol. 436, pp. 267/[1221]–279/[1233], 2005

ISSN: 1542-1406 print/1563-5287 online
DOI: 10.1080/15421400590955839

Measurement of Flexoelectric Coefficients in Nematic Liquid Crystals Using Shallow Grating Devices

Hanna M. Sykulska
Lesley A. Parry-Jones
Steve J. Elston
Department of Engineering Science, Oxford University, Parks Road, Oxford, United Kingdom

A nematic device with a shallow grating and homeotropic anchoring is used to probe the flexoelectric effect. Applying a sinusoidally varying voltage across the cell, the transmittance of the device between crossed polarisers is found to consist of a mixture of 1st and 2nd harmonics, corresponding to the flexoelectric and dielectric responses of the director to the applied electric field. The results are compared with theoretical ones generated using a 1-dimensional approximation to the cell structure, and a value for the sum of the flexoelectric coefficients determined.

Keywords: flexoelectricity; grating; harmonics; measurement; nematic

INTRODUCTION

The flexoelectric effect was first discussed by Meyer [1] in 1969, as being analogous to piezoelectricity (strain induced polarisation) in solids. Classically, the flexoelectric effect arises from the molecules of the liquid crystal having shape asymmetry as well as a permanent dipole. Deforming the director of the liquid crystal generates a spontaneous polarization which interacts with any electric field. Symmetry arguments show that splay and bend but not twist deformations can give rise to a polarisation [2].

A phenomenological formula for the flexoelectric polarization can be written as $P_f = e_1\mathbf{n}(\nabla\cdot\mathbf{n}) + e_3(\nabla\times\mathbf{n})\times\mathbf{n}$ [3] where e_1 and e_3 are the

HMS and SJE would like to thank the Leverhulme Trust, and LPJ the Royal Society, for funding.

Address correspondence to Lesley A. Parry-Jones, Department of Engineering Science, Oxford University, Parks Road, Oxford, OX1 3PJ, United Kingdom. E-mail: lesley.parry-jones@eng.ox.ac.uk

splay and bend flexoelectric coefficients. In practice, these flexoelectric coefficients tend not to be measured separately, but rather their sum or difference is often found.

De Gennes makes the point in his 1974 work [3] that 'to the extent flexoelectricity is a strong effect, the conventional local elastic theories are not correct.' Indeed, for most macroscopic elastic experiments, flexoelectric effects are probably weak enough that they can be forgotten. And in fact in static cases, ions do cancel out the voltage differences in the cell. However, there are regions where flexoelectric effects cannot be ignored. This is important since the flexoelectric effect provides a mechanism for switching which leads to bistability, for example the zenithally bistable nematic device (ZBN or ZBD). In the case of ZBD's the switching between the two stable ground states relies on the flexoelectric polarization to distinguish between positive and negative applied fields. This allows for the production of liquid crystal displays that use up to 100 times less energy.

Many experimental studied have attempted to observe and understand flexo-electro-optical properties. Different techniques have been suggested since the pioneering work of Prost and Marcerou [4] to observe the dipole mechanism. There have been a number of attempts to measure either the sum or the difference of these two coefficients as described in Chandrasekhar [5], and more recently by Edwards *et al.* [6] and Mazzulla *et al.* [7]. Jewel and Sambles [8] determined the response to AC and DC applied voltages of the director profile within a Hybrid Aligned Nematic liquid crystal cell. They used the optical wave-guide method known as the Fully-Leaky Guided Mode Technique and measured the sum of the splay and bend flexoelectric coefficients $(e_1 + e_3)$ of E7 to be $1.5 \times 10^{-11}\,\mathrm{Cm}^{-1}$. Unfortunately, the method used was complicated and time consuming. Edwards *et al.* [6] used a cell containing a diffraction grating to study the behaviour of the nematic liquid crystal E7. A flexoelectric term and weak anchoring was used to model the grating surface, and the flexoelectric term $(e_1 + e_3)$ determined as $2 \times 10^{-11}\,\mathrm{Cm}^{-1}$. At present there is no standard measurement technique for quantifying the flexoelectric effect. This paper investigates the flexoelectric effect and a potential way of measuring it reliably.

One of the problems of measuring the flexoelectric effect is that it is often masked by a much larger dielectric effect. Also problems may arise with low frequency measurements due to ionic drift. To overcome these problems, in this work we follow the method of Warrier and Madhusudana [9], and apply a sinusoidally varying field to a cell, and resolve the response into harmonics. Exploiting the fact that the flexoelectric effect depends on the applied electric field, whereas the dielectric effect depends on the square of the field, we can interpret first and second harmonics as due to the two different effects.

CELL GEOMETRY

In order to couple to the flexoelectric polarisation, homeotropically aligned devices with a shallow gratings on one surface were used. The gratings used in the cells were written into a photoresist using Argon Ion laser interferometry to give a 1 μm pitch and approximately 0.2 μm depth. A chromium complex was used as the surfactant to give homeotropic alignment on both the grating and substrate surfaces. The liquid crystal devices were filled with a commercial nematic liquid crystal mixture called E7, manufactured by Merck. The cell geometry is shown in Figure 1.

EXPERIMENT

In an external field, E, the flexoelectric effect leads to a free energy density $F = -P_f \cdot E$. Therefore the flexoelectric response is proportional to the electric field E and is dependant on its sign. This is different to the dielectric effect which varies as E^2. Applying a periodic electric field, e.g., of the form $E \propto \cos \omega t$, means that the dielectric response goes as $E^2 \sim \cos^2 \omega t \sim 1 + \cos 2\omega t$. Therefore the dielectric response is at frequency 2ω while the flexoelectric response is at frequency ω.

The device was placed between crossed polarisers with the grating of the device set at 45° to the polarisers, such that with no applied

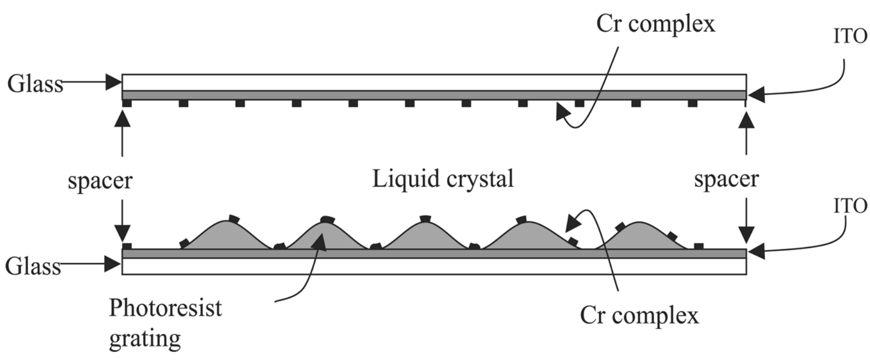

FIGURE 1 Schematic diagram of the cell geometry used to probe the flexoelectric effect. The cell was a homeotropically aligned device with a shallow grating on one surface.

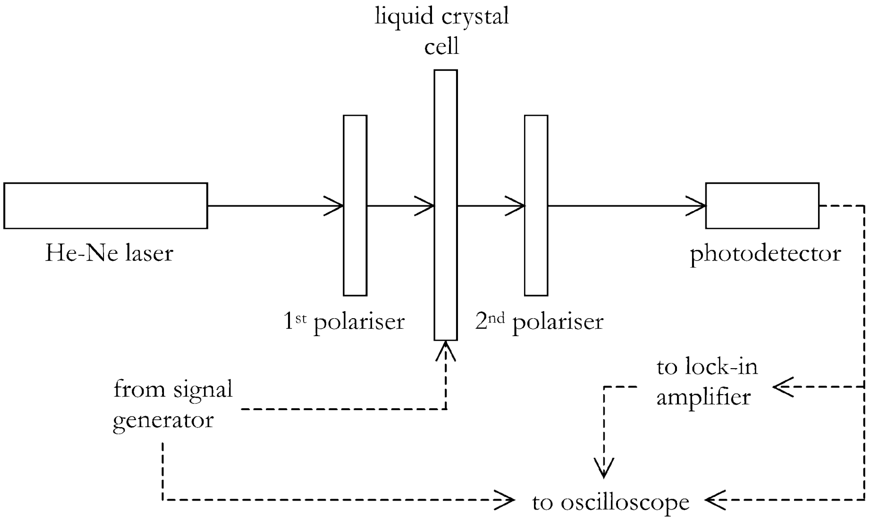

FIGURE 2 The apparatus set-up used to probe the flexoelectric effect. The device is place between crossed polarisers with the grating at 45° to the polarisers. A sinusoidally varying voltage is applied to the cell and the harmonics of the response extracted by the lock-in amplifier.

voltage, the device appeared bright (i.e., a normally bright setup). The set-up is shown in Figure 2. The light source used was a He-Ne laser which is highly monochromatic (632.8 nm). A sinusoidally varying electric field of different amplitudes is applied across the cell from a signal generator. The response consists of a mixture of 1st and 2nd harmonics, corresponding to the flexoelectric and dielectric responses of the director to the applied electric field. Using a sinusoidal field has the advantage of limiting ionic migration and allowing the flexoelectric and dielectric effects to be separated. The transmitted light was detected by the photodetector and transmitted as an electrical signal into a lock-in amplifier allowing the first and second harmonic of the responses to be separated. All measurements were preformed at a room temperature of around 20°C.

RESULTS

The waveform data in Figure 3 clearly shows a mixture of first and second harmonics.

The larger peaks are where the flexoelectric and dielectric terms are acting in the same direction, and the lower when they are acting in opposition.

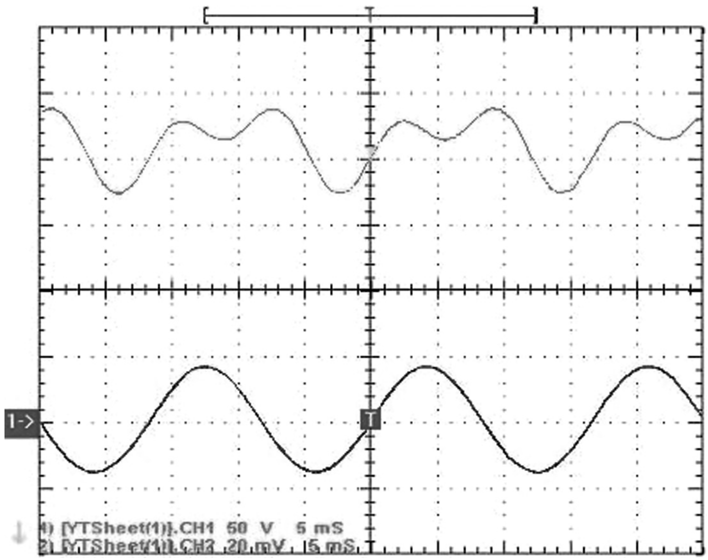

FIGURE 3 An input signal of 20 V, 60 Hz and the response through the cell showing a mixture of first and second harmonic. The lower curve is the signal applied to the cell and the upper curve shows the transmitted light through crossed polarisers.

Figure 4 shows the relative proportions of first and second harmonics as a function of the amplitude of the sinusoidal voltage. The results are shown for two different cells with different grating structures within them, and for a frequency of 60 Hz.

It is particularly clear in grating 1 that at low voltages, the flexoelectric response is proportional to E, whilst the dielectric response is proportional to E^2. This can be understood in terms of the relative contributions of these two effects to the total free energy density, as will be seen in the next section. In order to verify this we should find that:

$$\frac{\text{1st harmonic} + \text{2nd harmonic}}{\text{1st harmonic}} = \frac{aE + bE^2}{aE} = 1 + \alpha E,$$

and when we plot the data from grating 1 in this way, as shown in Figure 5, we do indeed get a straight line through (0,1).

Because the dielectric effect scales quadratically with the applied field, it dominates the flexoelectric effect for moderate fields >10 V. Both effects get smaller at high fields because the director is vertical for much of the applied voltage cycle, so the first and second harmonic responses diminish.

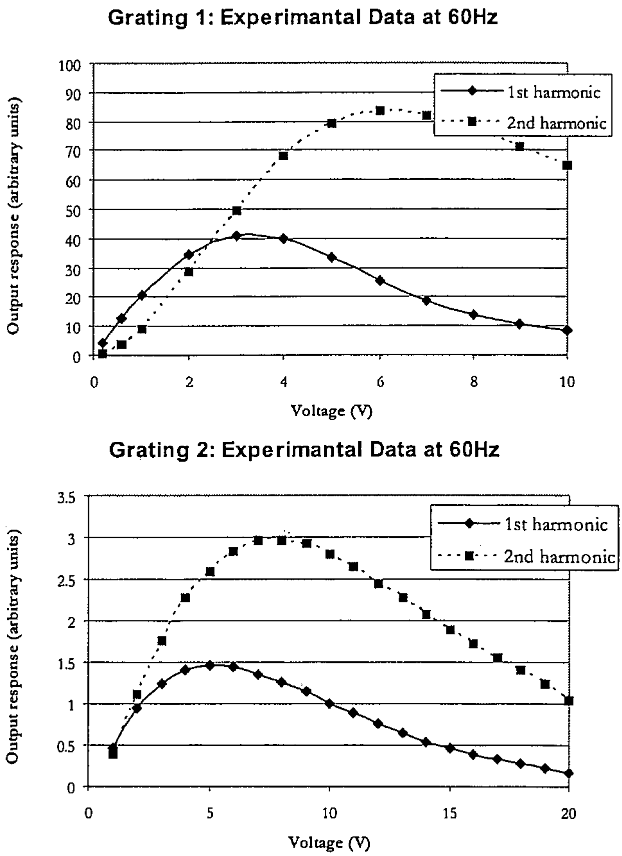

FIGURE 4 Experimental data from 2 gratings showing first and second harmonic response at 60 Hz. At larger fields the dielectric response dominates whereas at very small fields the flexoelectric response dominates.

MODELLING

The cell was modelled in two dimensions as a periodically repeating unit of the grating. The equilibrium profiles of the cell were found by minimising the free energy of the liquid crystal by solving the differential equations that model it. FlexPDE is a package for solving partial differential equations which uses a finite element method. The director profile through the cell was found in response to different electric fields applied across the device for a liquid crystal with a positive dielectric anisotropy. Two-dimensional modelling was possible as the director was assumed to stay in the plane of the cell (i.e., there is no twisting of the director involved).

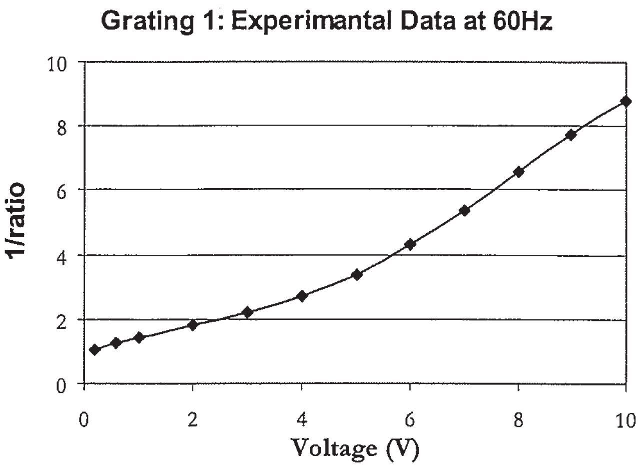

FIGURE 5 Data for grating 1 at 60 Hz showing (1st + 2nd)/1st. The data intercepts the vertical axis at 1, as predicted by theory.

Modelling the director structures in two dimensions we found that for a large proportion of the cell (the layer of liquid crystal far from the grating structure) the director is always vertical and unaffected by applied fields. Figure 6 shows the modelled director profile. This

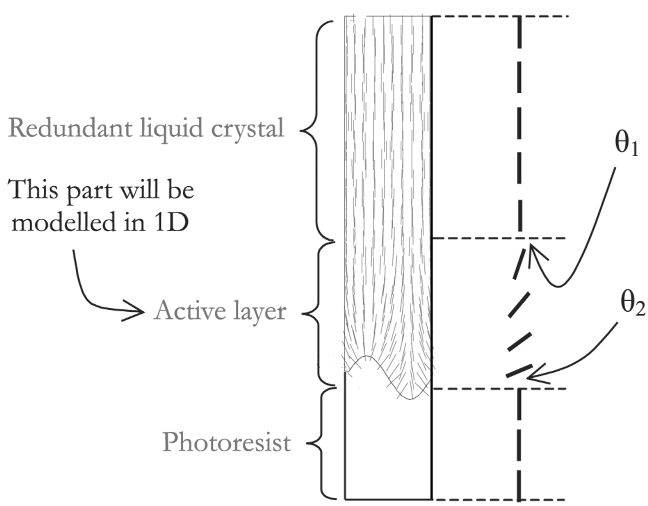

FIGURE 6 An annotated example of the result of two dimensional modelling for a cell with a grating with 5 V applied across the device.

suggests the 'active layer' of the liquid crystal is much thinner than the length of the cell.

1D MODEL

Both surfaces of the liquid crystal had homeotropic alignment; the top surface of the 'active layer' was anchored at an angle θ_1 to the surface, fixed at 90°. The effective angle at the grating surface θ_2 is not fixed but was modelled with an effective surface energy provided by the anchoring energy $F_s = W\sin^2(\theta - \theta_2)$, and an effective surface viscosity η_{surf}.

Considering the elastic constants separately for splay and bend, the Euler-Lagrange torque expression in one dimension is:

$$\eta\frac{d\theta}{dt} = (K_{11}\cos^2\theta + K_{33}\sin^2\theta)\frac{d^2\theta}{dz^2} + \frac{(K_{33}-K_{11})}{2}\sin 2\theta\left(\frac{d\theta}{dz}\right)^2 + \frac{1}{2}\varepsilon_0\Delta\varepsilon E^2\sin 2\theta - \frac{(e_1+e_3)}{2}\sin 2\theta\frac{dE}{dz}$$

Note that the flexoelectric coefficients occur as a sum (e_1+e_3) so the comparison of theory and experiment will lead to an evaluation of the sum of the flexoelectric coefficients. The electric field E would normally be calculated from the displacement field D using the following approach:

$$D = \varepsilon_0\varepsilon_z E + P_{flexo} \tag{1}$$

$$\begin{aligned}
-V &= \int E\,dz = \int \frac{D - P_{flexo}}{\varepsilon_0\varepsilon_z}dz \\
&= \frac{D}{\varepsilon_0}\int\frac{dz}{\varepsilon_z} - \frac{(e_1+e_3)}{\varepsilon_0}\int\frac{\sin\theta\cos\theta\frac{d\theta}{dz}}{\varepsilon_\parallel\sin^2\theta + \varepsilon_\perp\cos^2\theta}dz \\
&= \frac{D}{\varepsilon_0}\int\frac{dz}{\varepsilon_z} - \frac{(e_1+e_3)}{2\varepsilon_0\Delta\varepsilon}\ln\left[\frac{\varepsilon_{z=d}}{\varepsilon_{z=0}}\right] = \frac{D}{\varepsilon_0}\int\frac{dz}{\varepsilon_z} - A
\end{aligned}$$

$$D = \frac{\varepsilon_0(A - V)}{\int\frac{dz}{\varepsilon_z}} \tag{2}$$

and then the electric field E is calculated as a function of position across the cell using equations [1] and [2]. However, in our model, we have made a very simple assumption to take account of the presence of ionic impurities in the cell. We know that the action of ionic impurities over large time scales is to cancel out any net polarisation present in the cell. Since the applied voltage in our model is DC balanced, such a net polarisation can only be of flexoelectric origin. We therefore assume that the time averaged flexoelectric polarisation is completely cancelled out by the ionic impurities. However, we assume that the ions cannot respond on the time scale of the applied voltage, and hence a flexoelectric polarisation is present temporarily. The calculation of the electric field profile in the cell is therefore modified as follows:

$$D = \varepsilon_0\varepsilon_z E + P_{flexo} + P_{ions} \qquad \text{where} \qquad P_{ions} = -\langle P_{flexo}\rangle$$

$$-V = \int E dz = \int \frac{D - P_{flexo} - P_{ions}}{\varepsilon_0\varepsilon_z} dz = \frac{D}{\varepsilon_0}\int\frac{dz}{\varepsilon_z} - A - \frac{1}{\varepsilon_0}\int\frac{P_{ions}}{\varepsilon_z}$$

$$D = \frac{\varepsilon_0(A - V + \frac{1}{\varepsilon_0}\int\frac{P_{ions}}{\varepsilon_z}dz)}{\int\frac{dz}{\varepsilon_z}}. \tag{3}$$

It is clear that in the case where the applied voltage is zero, so that $P_{ions=} - P_{flexo}$, the integral in the numerator of the expression for D in equation [3] is equal to $-A$, and hence $D = 0$, unlike the case when there are no ions, there is a net displacement field even with no applied voltage.

A finite anchoring energy and viscosity was allowed at the grating surface, giving the following torque equation for the surface:

$$\eta_{surf}\frac{d\theta_{surf}}{dt} = (K_{11}\cos^2\theta_{surf} + K_{33}\sin^2\theta_{surf})\frac{d\theta}{dz}\bigg|_{surf}$$
$$- W\sin(2(\theta_{surf} - \theta_2)) - (e_1 + e_3)\sin 2\theta_{surf}E_{surf}.$$

These equations are not trivial to solve analytically so a numerical method to model the device was employed.

The cell was modelled in one dimension in C++ and a sinusoidally varying voltage applied. At each moment in time the program finds the director distribution through the cell and the optics subroutine finds the transmission between crossed polarisers using a Jones matrix approach. As the voltage goes through cycles, the transmission is obtained as a function of time. After each voltage cycle the first and second harmonics are calculated and the program stops when the harmonics have stopped changing. A trace of the modelled time-dependant transmission is shown as a function of time in Figure 7.

FITTED PARAMETERS

The modelled data was compared to the experimental results and the best fit provided by the covariance of the variable parameters in the

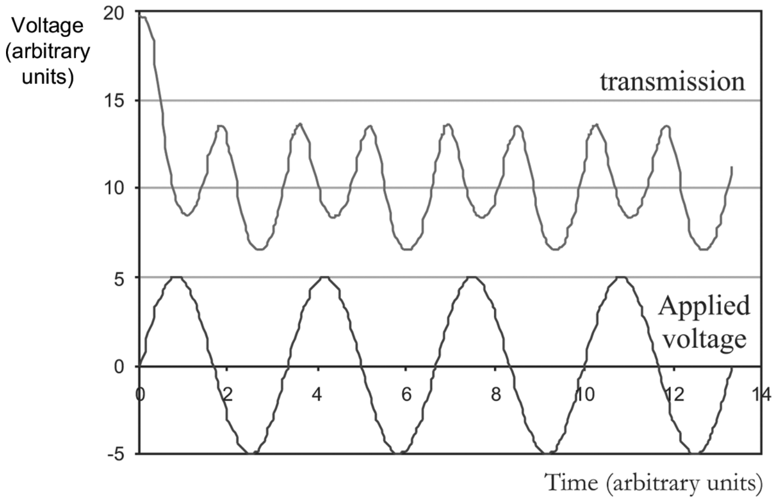

FIGURE 7 The dynamic response of the cell was modeled using a finite difference approximation. The program ran at each oscillating voltage until the transmission gave a stable response. The lower curve is the signal applied to the model and the upper curve shows the transmitted light through crossed polarisers as predicted by the model.

equations that describe the behaviour of the liquid crystal; the flexoelectric coefficient, the surface anchoring energy and the effective angle at grating surface (See Figure 8). The values for the viscosity, elastic constants and dielectric permittivity of the liquid crystal were set equal to values reported by Merck for E7:

$$\begin{aligned} \eta &= 0.19\,\text{Pa s}, \\ K_{11} &= 11.7\,\text{pN}, \\ K_{33} &= 17.1\,\text{pN}, \\ \Delta\varepsilon &= 14.3, \end{aligned}$$

and kept fixed as the other parameters were varied. The parameters that the program predicts for each grating are shown and discussed below.

Flexoelectric Coefficient

For both gratings 1 and 2, the flexoelectric coefficient generated $(e_1 + e_3)$ was $(4 \pm 0.5) \times 10^{-11}\,\text{Cm}^{-1}$. The values are similar in order of magnitude to those previously measured by the Exeter group in

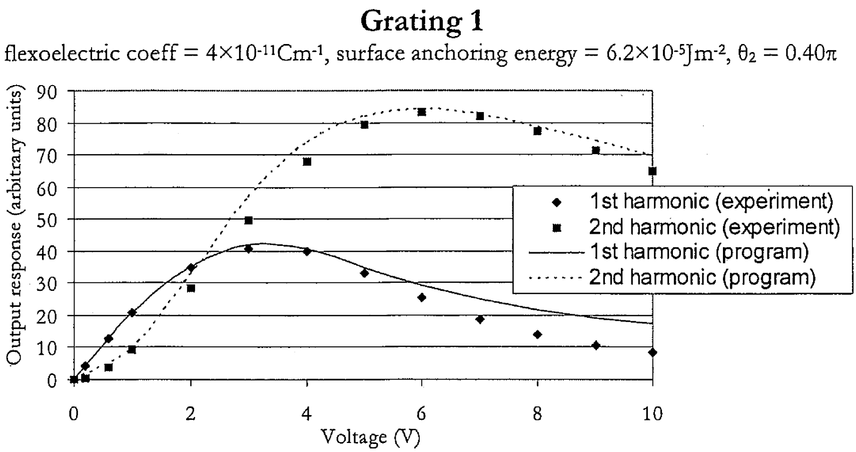

(a)

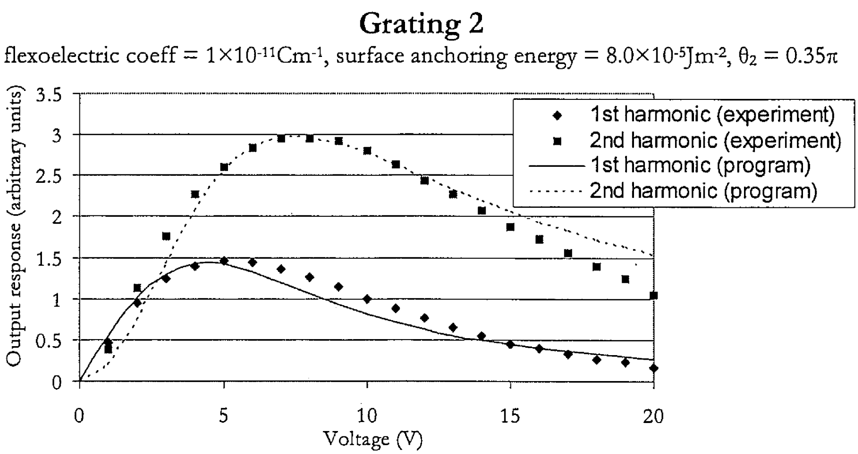

(b)

FIGURE 8 The best match to the real data that the model provides for (a) grating 1 and (b) grating 2. The fitting provides values for the variable parameters of the modelling equations as shown for each grating.

5CB [7] and E7 [8], $3.0 \times 10^{-11}\,\mathrm{Cm}^{-1}$ and $1.5 \times 10^{-11}\,\mathrm{Cm}^{-1}$ respectively. We believe that the reason that our measurement is slightly higher is due to the approximations involved in using a 1D model to simulate a structure that is truly 2D. It is likely to be the case that gradients in the electric field in the direction along the grating wavevector (ignored in the model presented here) are as large as those in the direction across the cell gap (included in our 1D model). Since it is this electric field gradient that determines the magnitude of the flexoelectric torque, it is clear that our method will provide an overestimate of the sum of the flexoelectric coefficients.

Surface Anchoring

For both gratings 1 and 2, the surface anchoring strength W was found to be $\approx (8 \pm 2) \times 10^{-5}\,\mathrm{Jm}^{-2}$. Literature records the value of W to be of the order of $5 \times 10^{-5}\,\mathrm{Jm}^{-2}$ [10,11]; these values seem reasonable for a homeotropic surface.

Effective Angle at Grating Surface

For both gratings, $\theta_2 = 0.25\pi$ and this value corresponds to an average value giving a grating depth of about 0.6 μm (calculated by treating the grating as a sine wave). These values are consistent with the exposure times used in the grating fabrication process.

CONCLUSIONS

The method uses shallow grating devices to separate the dielectric and flexoelectric effects by observing the first and second harmonics of the transmission of a laser through crossed polarisers while applying a sinusoidal voltage to the cell. Using this method, it was found that the flexoelectric effect was more dominant at smaller voltages.

The experimental data derived through the above method was compared to theoretical computer models of the behaviour of such a liquid crystal device. To model the cell dynamically, a 1d model written in C ++ was created and its predictions were compared to experimental data. The comparison allowed the deduction of the flexoelectric coefficients $(e_1 + e_3)$ which were measured for two different gratings. For both gratings this gave a value of $(4 \pm 0.5) \times 10^{-11}\,\mathrm{Cm}^{-1}$, which is comparable to (but slightly higher than) documented measured values [6–8]. We understand that by approximating a 2D grating device with a 1D model we overestimate the flexoelectric coefficient and hence propose to use truly 1D systems (e.g., HAN cells) in our future work.

REFERENCES

[1] Meyer, R. B. (1969). *Phys. Rev. Lett.*, *22*(18), 918.
[2] Rudquist, P. & Lagerwall, S. T. (1997). *Liq. Cryst.*, *23*, 503.
[3] De Gennes, P. G. (1974). *The Physics of Liquid Crystals*, Clarendon: Oxford.

[4] Prost, J. & Marcerou, J. P. (1977). *J. Phys (Paris)*, *38*, 315.
[5] Chandrasekhar, S. *Liquid Crystals*, 205.
[6] Edwards, E. G., Brown, C. V., Kriezis, E. E., & Elston, S. J. (2003). *Mol. Cryst. Liq. Cryst.*, *400*, 13–19.
[7] Mazzulla, A., Ciuchi, F., & Sambles, J. R. (2001). *Physical Review E*, *64*, 021708.
[8] Jewell, S. A. & Sambles, J. R. (2002). *Journal of Applied Physics*, *92*(1), 19–24.
[9] Warrier, S. R. & Madhusudana, N. V. (1997). *Journal de Physique II*, *7*, 1789.
[10] Cognard, J. (1982). *Mol. Cryst. Liq. Cryst.*, Suppl. 1.
[11] Bahadur, B. (Ed.) (1992). *Liquid Crystal Applications and Uses*, World Scientific Publishing Co. Pte. Ltd., Vol. 3.